Precision and Accuracy of Satellite Radar and Laser Altimeter Data Over the Continental Ice Sheets

Anita C. Brenner, John P. DiMarzio, and H. Jay Zwally

***Abstract*—The unprecedented accuracy of elevations retrieved from the Ice Cloud and Land Elevation Satellite (ICESat) laser altimeter is investigated and used to characterize the range errors in the Environmental Satellite (Envisat) and European Remote Sensing 2 Satellite (ERS-2) radar altimeters over the continental ice sheets. Cross-mission crossover analysis between time-coincident ERS-2-, Envisat-, and ICESat-retrieved elevations and comparisons to an ICESat-derived digital elevation map are used to quantify the radar elevation error budget as a function of surface slope and to investigate the effectiveness of a method to account for the radar altimeter slope-induced error. The precision and accuracy of the elevations retrieved from the ICESat Geoscience Laser Altimeter System and the European Space Agency radar altimeters on ERS-2 and Envisat are calculated over the Greenland and Antarctic ice sheets using a crossover analysis. As a result of this work, the laser precision is found to vary as a function of surface slope from 14 to 59 cm, and the radar precision varies from 59 cm to 3.7 m for ERS-2 and from 28 cm to 2.06 m for Envisat. Envisat elevation retrievals when compared with ICESat results over regions with less than 0.1° surface slopes show a mean difference of 9 ± 5 cm for Greenland and -40 ± 98 cm over Antarctica. ERS-2 elevation retrievals over these same low surface slope regions differ from ICESat results by -56 ± 72 cm over Greenland and 1.12 ± 1.16 m over Antarctica. At higher surface slopes of 0.7° to 0.8°, the Envisat/ICESat differences increase to -2.27 ± 23 m over Greenland and to 0.05 ± 26 m over Antarctica.**

***Index Terms*—Altimetry, ice, laser measurements, radar altimetry, remote sensing.**

I. Introduction

SATELLITE altimetry over the continental ice sheets has proven to be a valuable tool in studying decadal ice sheet mass balance changes by yielding measurements of elevation changes over the past 26 years over Greenland and Antarctica [1]–[3]. Since 1991, we have had continuous coverage of all of Greenland and Antarctica to 81.5° south by the European Space Agency (ESA) radar altimeters on the European Remote Sensing Satellites (i.e., ERS-1 and ERS-2), and Environmental Satellite (ENVISAT). In 2003, the Ice Cloud and Land Elevation Satellite (ICESat) was launched by the National Aeronautics and Space Administration (NASA) carrying the Geoscience Laser Altimeter System (GLAS) instrument [4]. GLAS has three lasers, each of which was projected to last a period of 1–1.5 years and give a precision of under 20 cm over the continental ice sheets. Problems with the first two lasers occurred, which have forced changes to the mission operations plan. Instead of operating continuously, the remaining lasers have been powered on and off at three- to six-month intervals to maximize the use of the ICESat mission for elevation change studies. The existing ICESat data set, with its unprecedented accuracy and precision, is now a valuable tool for quantifying the accuracy and improving the interpretation of the radar altimetry measurements.

TABLE I
SUMMARY OF THE DATA USED IN THIS PAPER

Mission	Time span in 2003	Mode	Waveform bin resolution (cm)	Source
ERS-2	2/21-3/31	ice mode	174	UK-PAF
ICESat/Laser 1	3/5-3/21	NA	15	Release 18
ENVISAT	10/1-11/31	fine mode	46	ESA SGDR
ICESat/Laser 2a	9/25-11/18	NA	15	Release 21

Most previous validations of radar altimetry have used airborne laser data [5] and *in situ* measurements, both of which have limited geographic coverage. Recently, GLAS data have been used to access the accuracy of Antarctic digital elevation maps (DEMs) produced mostly from radar altimetry [6]. In this paper, we compare the very precise ICESat data, which cover large portions of Greenland and Antarctica with time-coincident ERS-2 and Envisat data giving a maximum limit to the residual errors remaining in the radar-retrieved elevations. The differences in the radar- and laser-retrieved elevations include errors in the radar retrievals due to inaccurate modeling of surface penetration, the slope-induced error caused by the large radar footprint, and limitations in the ability of the processing algorithm to retrieve a precise geolocated elevation. The major errors in the laser retrieval are due to inaccurate modeling of the saturation and forward scattering affects on the return and the inaccuracies in the retrieved laser pointing angle. The slope-induced error in the laser retrievals is not a concern because of the narrow divergence of the laser beam. The radar altimeters cannot maintain track over regions of large surface slope; however, they measure through all atmospheric conditions. The laser altimeter can measure over all ice sheet surfaces, but it cannot measure through thick clouds.

This paper uses a crossover analysis with intramission passes to calculate the relative accuracy or precision of height

Manuscript received June 6, 2006; revised August 14, 2006. This work was supported in part by the National Aeronautics and Space Administration Cryosphere Program and in part by the Ice Cloud and Land Elevation Satellite Project Scientist.

A. C. Brenner is with Science Systems and Applications, Inc., Lanham, MD 20706 USA (e-mail: Anita_Brenner@ssaihq.com).

J. P. DiMarzio is with Stinger Ghaffarian Technologies, Inc., Greenbelt, MD 20770 USA (e-mail: john.p.dimarzio@gsfc.nasa.gov).

H. J. Zwally is with the National Aeronautics and Space Administration, Goddard Space Flight Center, Greenbelt, MD 20771 USA (e-mail: H.J.Zwally@nasa.gov).

Digital Object Identifier 10.1109/TGRS.2006.887172

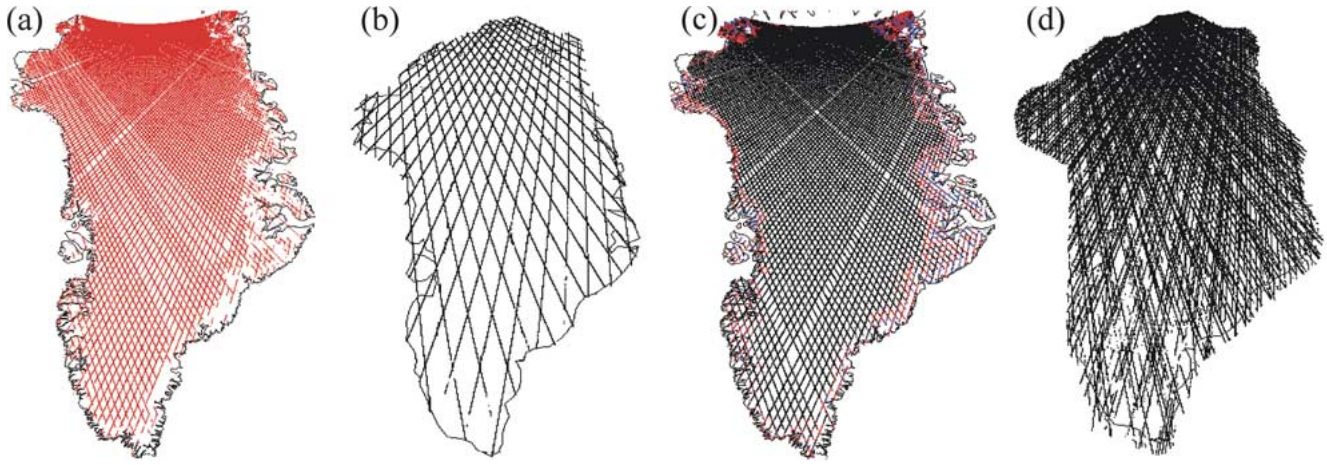

Fig. 1. Data used for the Greenland portion of the study. Black is ICESat or Envisat fine mode. Red is ERS-2 ice mode or Envisat medium-resolution mode, and blue is Envisat coarse mode. (a) ERS-2. (b) ICESat Laser 1. (c) Envisat. (d) ICESat Laser 2a.

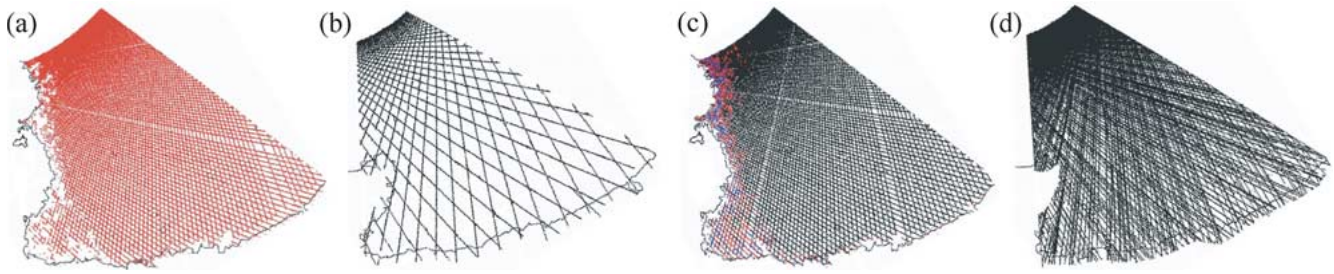

Fig. 2. Segment of the data used for the Antarctica portion of the study. Black is ICESat or Envisat fine mode. Red is ERS-2 ice mode or Envisat medium-resolution mode, and blue is Envisat coarse mode. (a) ERS-2. (b) ICESat Laser 1. (c) Envisat. (d) ICESat Laser 2a.

elevations retrieved from ERS-2, Envisat, ICESat Laser 1, and ICESat Laser 2a measurements. This procedure also yields an accuracy calculation from crossovers over the nonsloping regions. The accuracy of the radar altimeter relative to the laser is calculated from intermission crossovers using time-coincident radar- and laser-retrieved elevations. A quantitative measurement of the difference between ERS-2- and Envisat-retrieved elevations over the continental ice sheets as a function of surface slope, as processed with the NASA Goddard Space Flight Center (GSFC) algorithms, is achieved by direct comparison between ERS-2 and Envisat and by comparing them individually to the ICESat-retrieved elevations. In addition, a quantitative evaluation of the effectiveness of the radar altimeter slope-induced error correction is carried out using the radar–laser intermission crossovers and by comparing the radar-retrieved elevations to an ICESat-derived DEM. In this paper, we investigate the precision and accuracy of the laser- and radar-retrieved elevations using the GSFC retrackers and radar slope correction procedures. Other approaches have been used by other investigators and will produce different results.

II. Data Description

ICESat Laser 1 operated from February 20 to March 29, 2003, for which time-coincident ERS-2 ice sheet data were also obtained. The Envisat data over the ice sheets for this time period have not yet been distributed to the authors. ICESat Laser 2 operated from September 25 to November 19, 2003, and will be referred to as Laser 2a. ESA has distributed the time-coincident Envisat data for the Laser 2a time period; however, the ERS-2 altimeter was no longer operating over the ice sheets. A summary of the data used in this paper is given in Table I.

Fig. 1 shows ground tracks of the data used over Greenland. Ground tracks for only a portion of Antarctica are shown in Fig. 2 to see more detail; however, all data over the entire continent of Antarctica were used in this paper. As shown in Figs. 1(a) and 2(a), the ERS-2 altimeter is always in ice mode over the ice sheets for the time period used. The sparseness of the Laser 1 coverage is clearly shown in Figs. 1(b) and 2(b), which is due to the eight-day repeat orbit. In Figs. 1(c) and 2(c), the Envisat ground tracks show how the altimeter stays in fine mode over the majority of the ice sheets, switching to medium resolution and then coarse resolution along the rougher steeper coastal and mountainous regions. For Laser 2a shown in Figs. 1(d) and 2(d), the ground tracks show the higher density of coverage due to the combination of both an 8-day and 45 days of a 91-day orbital repeat. The data are described in more detail in the following sections.

A. Data Source

The source for ERS-2 data is the United Kingdom Processing and Archiving Facility waveform analysis product tapes. The source for Envisat data is the ESA Sensor Geodetic Data Records. The ICESat Laser 1 data are release 18 and the Laser 2a data are release 21, both of which were obtained from the GLAS Science Computing Facility at NASA/GSFC and are available at the National Snow and Ice Data Center.

B. Corrections

All data are corrected for tropospheric delay by integrating the refractivity as a function of pressure, temperature, and relative humidity, along the ray path [7]. The climatology used for the calculation is obtained from the six hourly global 1° fields released by the National Center for Environmental Prediction. Over the polar regions, the root-mean-square (rms) delay error for the dry portion is less than 12 mm for both laser and radar path delay. The rms delay error for the wet portion is less than 0.15 mm for laser [4] and less than 1 cm for radar. The solid Earth tides and equilibrium long-period tides are computed using the same models used by the TOPEX/Poseidon mission [8]. Corrections specific to radar or laser are discussed in the following sections.

C. Radar Altimeter Data

Both ERS-2 and Envisat were in 35-day repeat-cycle orbits with a maximum latitudinal coverage of $\pm 81.5^\circ$. The measurement rate was 20 Hz, giving a measurement every 330 m along the ground track. The beam-limited footprint varied from 1.2 to 16 km in diameter, increasing with surface slope and roughness. The Envisat radar altimeter operated in three range resolution modes, automatically changing between modes based on the onboard tracker algorithm. These are fine (320 MHz), medium (80 MHz), and coarse (20 MHz) modes, each providing a $4\times$ expansion of the range window to allow tracking over rough and highly sloped surfaces. As shown in Figs. 1 and 2, most of the Envisat data over the ice sheets are in fine mode, and almost all of the data spatially coincident with ERS-2 are in fine mode. Therefore, we use only the Envisat fine-mode data in this paper. The ERS-2 altimeter for the time periods used was operated only in ice mode over the ice sheets, which is comparable to the Envisat medium-resolution mode.

The ESA radar altimeter onboard tracker is designed to robustly follow the changing ice sheet surfaces and does not keep the ramp of the return centered over the "tracking gate" to which the telemetered range is measured. To calculate precise elevations from ESA radar altimetry, on-ground retracking is required. Both ESA and NASA have developed specialized ice sheet retrackers that are optimized for the ice sheet surfaces. This paper uses the GSFC Version 4 (V4) retracking algorithm for ERS-2 and Envisat elevation retrieval. This algorithm is optimized for ice sheet radar returns; however, the retracked range error can be significant (on the order of meters), especially over rougher regions where multiple surfaces in the footprint cause multiple ramps in the return [9].

The ice sheet return from radars is a composite of surface scattering and subsurface volume scattering due to penetration of the microwave signal [10] as shown in Fig. 3. Penetration varies with surface characteristics, and for microwave altimetry, it has been shown to be as much as 4.7 m in the cold dry regions [11]. The GSFC V4 retracker is designed to pick up multiple reflective surfaces within the footprint by using either a single-ramp function or a double-ramp function to fit the return, automatically switching between the two functions based on the return waveform shape. The "tracking" location is always taken to the midpoint of the first ramp. This can help assure

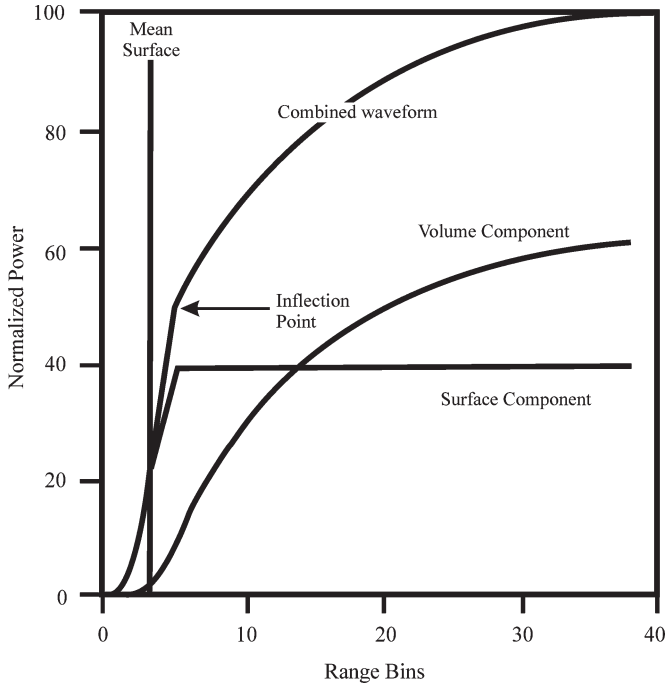

Fig. 3. Radar return over ice sheets is a combination of a surface component with a subsurface volume scattering component due to penetration. The mean surface elevation is measured to the midpoint of the ramp of the surface component [10].

the selection of the surface return when volume scattering is present. Switching between functions also has the possibility of causing "tracker jitter." A significant portion of the ERS-2 ice mode returns are fit using a double-ramp function. For Envisat, over 99% of the waveforms are fit using a single-ramp function, and inspection of the returns shows that there is no discernable double ramp.

Another commonly used retracker for radar altimetry is a simple threshold retracker [12], [13]. The threshold retracker selects the location on the return where the power is a certain percentage of the maximum power after accounting for the noise level. Davis [13] showed that the threshold retracker reduces the standard deviation of the crossovers when comparing results from different time periods over that of the GSFC V4 retracker.

The effect of penetration on the retrieved elevation is retracker dependent [14], [15]. Ridley and Partington [10] found the GSFC V4 retracker to be more insensitive to the effects of penetration and subsurface volume scattering and, therefore, to be more accurate than a threshold retracker in their presence. This is because the second ramp starts near the point of inflection at the end of the rise from the surface scattering function, so that the midpoint of the first ramp represents the range to the surface. The threshold retracker, however, is directly dependent on the maximum power, which increases in the presence of subsurface scattering. The threshold retracker is useful for elevation change studies because it gives less noisy results, but a functional retracker such as the GSFC V4 is more appropriate when an absolute elevation is required.

Elevation retrievals are retracker dependent, and the results are always shown for the GSFC V4 retracker. To show the effect of the different retrackers, where appropriate, results are also

given using a 10% threshold retracker and using only retrievals from the GSFC V4 single-ramp waveform data.

The International Reference Ionosphere 95 model [16] is used for the radar ionospheric path delay. Since the total electron content of the atmosphere diminishes in the polar regions, the error is less than 1 cm under normal conditions and less than 2 cm during high solar activity.

Over sloping surfaces, usually the largest error in the elevations retrieved from the radar altimeter range measurements is the slope-induced error caused by the large size of the beam-limited footprint [17], [12]. The measurement is the range to the closest point within this footprint, which is not the subsatellite location over sloping irregular topography. In fact, there can be ambiguity in where the measurement is coming from if two or more reflective surfaces within the larger footprint are at the same elevation. Either relocating the range to the closest point within the footprint or correcting the range while leaving the geolocation at the subsatellite point can account for this error. Both methods are limited by the accuracy of the *a priori* knowledge of the topography.

The GSFC range correction method assumes a planar surface over the beam-limited footprint. Using small angle assumptions, the correction becomes a function of the altitude and the slope squared as given by

$$\Delta R_{\text{slope}} = \frac{H \times \alpha^2}{2} \tag{1}$$

where H is the altitude of the satellite above the surface (in meters), and α is the slope of the surface (in radians).

The magnitude of this correction for the ESA radar altimeters varies from 2.5 m at slopes of 0.1° up to 250 m for slopes of 1.0°.

D. Laser Altimeter Data

ICESat data cover the ice sheets between $\pm 86^\circ$. For Laser 1, ICESat flew in an 8-day repeat orbit. For Laser 2a, one 8-day repeat orbit was flown followed by 43 days of a 91-day repeat orbit. GLAS takes 40-Hz measurements, which yield a data point, every 170 m along the satellite ground track over a small $\sim$70-m footprint. The full signal from the spacecraft to the ground and back is digitized at a resolution of 15-cm bins, which is a factor of 3 better than the finest mode of the radar altimeter.

The largest error source in calculating the elevation from each ICESat measurement is the precision of the pointing knowledge of the laser beam. The Laser Reference System (LRS) is a major input required to precisely calculate the beam pointing angle. For Laser 1, the LRS was only operating during a portion of most orbits. For Laser 2a, the LRS operated continuously. The Laser 2a LRS signature was used to help model the LRS for Laser 1 pointing angle determination. Release 18 of ICESat Laser 1 data was created using the modeled LRS. Release 21 of GLAS Laser 2a used the same processing algorithms as release 18, and a precision attitude was calculated using the measured LRS data as well as laser scan maneuver calibrations [18], which were not performed during Laser 1. The pointing knowledge accuracy is 1.6 ± 3.2 arcsecond for Laser 1 release 18 and 0 ± 1.3 arcsecond for Laser 2a release 21 [18]. The GLAS science team is still improving the pointing knowledge precision, and later releases should show related improvement in elevation precision.

Two other sources of error in laser altimetry are: 1) forward scattering caused by thin clouds and low-level atmospheric effects; and 2) saturation from high-energy returns over bright smooth flat surfaces, both of which cause centimeters to meters of ranging errors. ICESat data with a gain of greater than 30 counts were not used in an attempt to remove measurements affected by clouds. Highly saturated returns with amplitudes greater than 220 counts for more than five consecutive samples were also removed. As with the radar altimeter returns, the laser returns must be retracked. The laser retracking algorithm fits a Gaussian to the return waveform. The range to the centroid of the Gaussian is used to calculate the elevation [19]. The Gaussian fitting reduces the error caused by forward scattering but does not completely remove it. The laser does not penetrate the surface; thus, there is no corresponding penetration error.

There is no measurable ionospheric path delay at the laser frequency, nor is there any slope-induced error due to the small divergence of the laser beam [20].

The ICESat validation results over the flat region of the Salar de Uyuni, Bolivia [21], compare GLAS results to a DEM formed by ground global positioning system (GPS) measurements. The rms of the differences was 4.9 cm with a mean value of 9.6 cm for Laser 2a. There are no absolute validation results over the ice sheets.

III. Methodology

This paper uses a crossover analysis to calculate the precision and accuracy of the elevations retrieved from the altimeter range measurements. Precision is calculated as the standard deviation of the crossover residual distribution. The accuracy is defined for this paper as the standard deviations over the flat smooth regions.

A. Radar Slope-Induced Error Correction

The GSFC slope-induced range correction is calculated using (1) with the slope values derived from a 10-km DEM, which is produced using the GEOSAT and ERS-1 geodetic mission data created with the same methodology as the 5-km DEM [9]. The 10-km DEM is used to obtain an average slope over the large radar footprint to minimize the chance of overcorrecting the data. The correction is added to the range measurement before the elevation is derived. The elevation geolocation is defined as the subsatellite location.

B. Crossover Analysis

A crossover residual is the difference in elevation calculated by two passes that cross over the same location [9]. The location of the crossover is calculated by fitting the latitude versus longitude coordinates of each pass to a quadratic function and calculating the intersection of the two functions. First, the crossover location is estimated by fitting the function to all data in the two ice sheet passes that cross each other. Then,

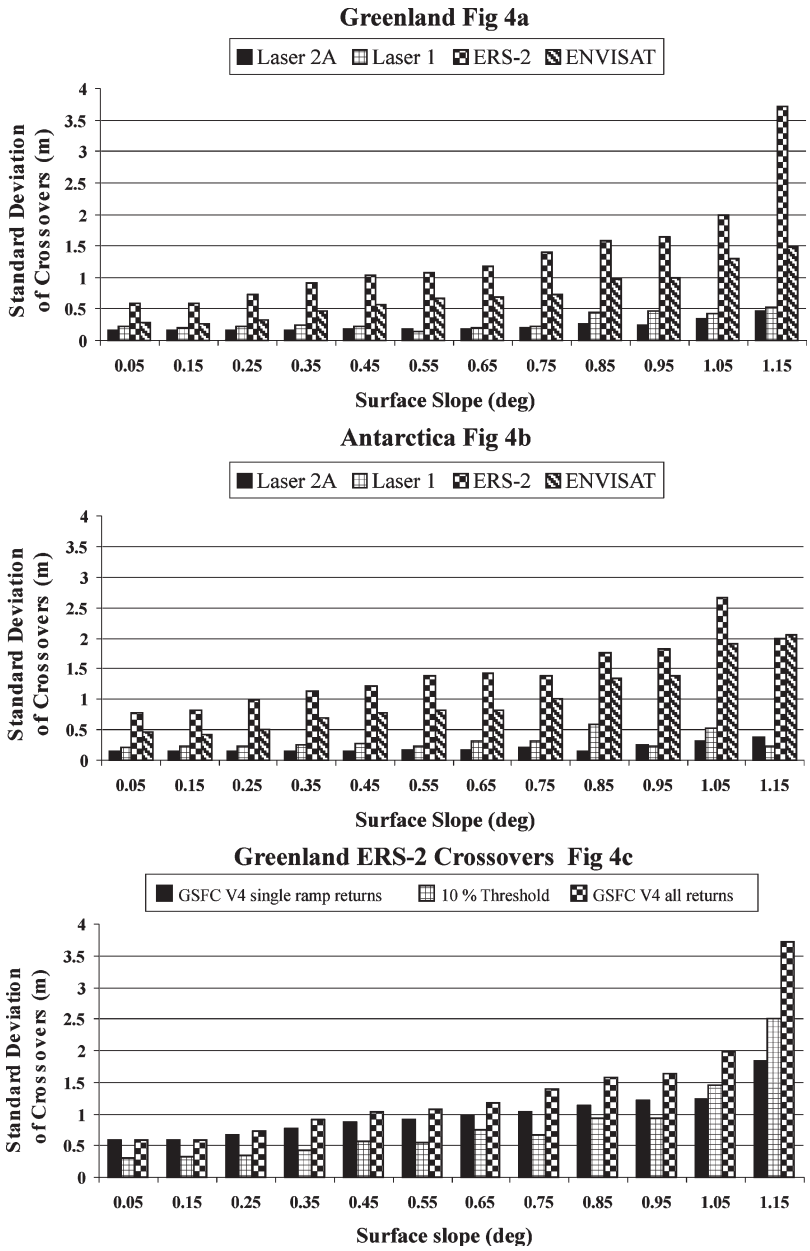

Fig. 4. Laser and radar altimeter elevation precision as a function of slope as measured by the standard deviation of the intramission crossover residuals. (a) Greenland. (b) Antarctica. (c) Results using different retracking scenarios over Greenland: GSFC V4 retracker with single-ramp returns only and the 10% threshold retracker. The GSFC V4 retracker results using data from both single- and double-ramp returns are repeated in (c) from (a) for comparison.

only data close to the crossover location are used, and the location is refined. The elevation at the crossover is calculated by linearly interpolating from the elevations on each side of the location for each pass. If valid elevations do not exist on both sides of the crossover within the expected distance (330 m for ERS-2 and Envisat and 170 m for GLAS), then the crossover is discarded. The crossover residual is the difference in the interpolated elevations from the two passes. The mean and standard deviation σ of a set of crossover residuals is calculated using a 3σ iterative convergent edit to remove outliers. Convergence is defined when the current value of σ agrees to the previous value to within 2%.

The precision of each mission is calculated as the standard deviation of a set of intramission elevation residuals at crossovers that are within 30 days of each other. As verified by the laser altimeter results (Section IV-A), the elevation differences over these surfaces over the 30 days have a mean of < 2 cm over all slopes and a standard deviation that differs from 14 cm at lower slopes to 59 cm at slopes between 1.1° and 1.2°.

The crossover statistics vary with surface slope. Therefore, all crossover residual statistics are calculated for ranges in surface slope from 0.0° to 1.2° in increments of 0.1°. The slope in this instance is calculated from the NASA/GSFC 5-km DEMs created from GEOSAT and ERS-1 geodetic mission radar data [9].

The precision of ERS-1, Envisat, and ICESat Laser 2a is also calculated as a function of location by taking the standard deviation σ of the intramission crossovers within each 50 $\times$ 50 km region over Antarctica. To remove outliers, the same type of 3σ iterative convergent edit defined previously is used.

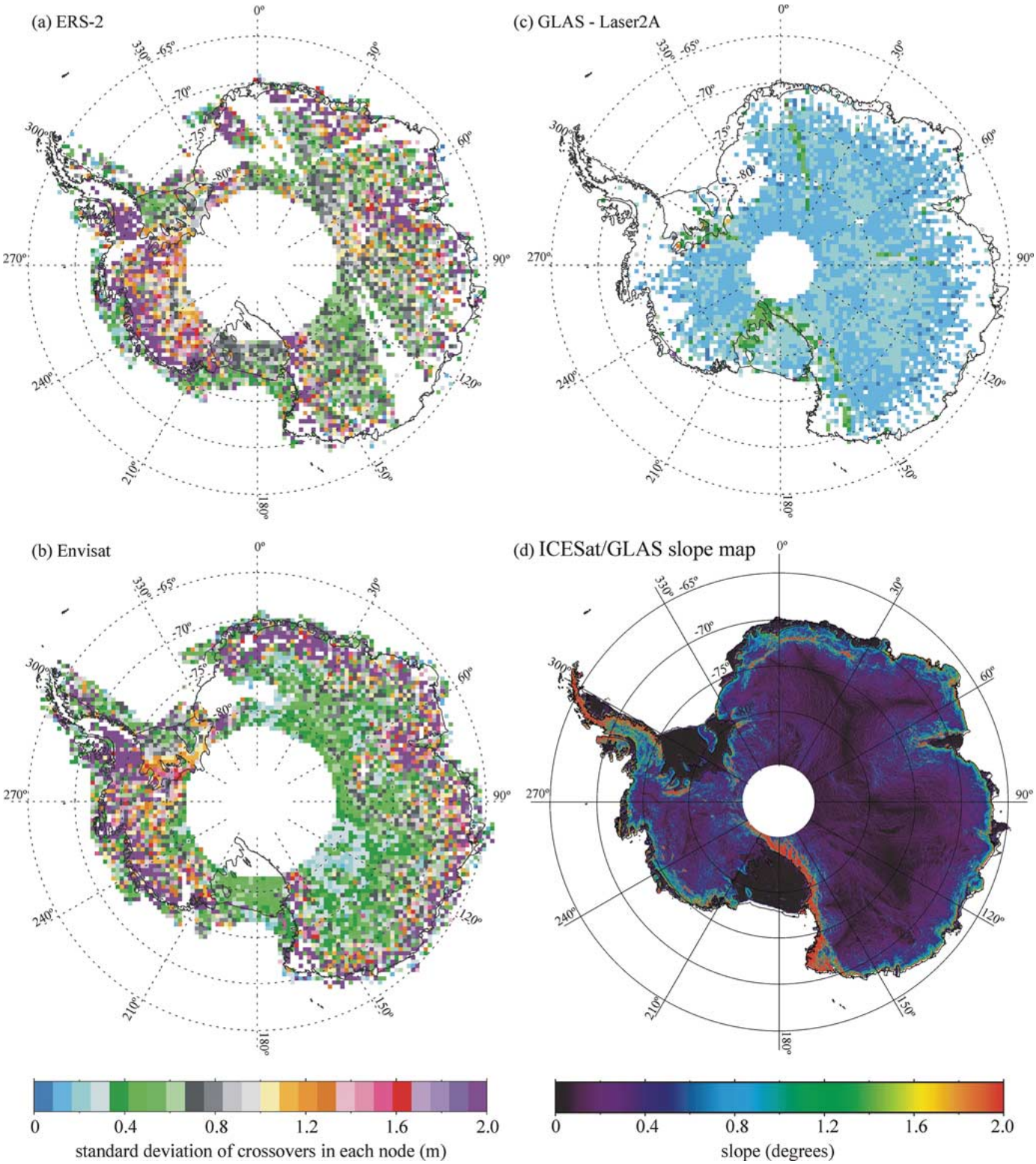

Fig. 5. Geographic representation of laser and radar altimeter elevation precision over Antarctica calculated from the standard deviation of all intramission crossover residuals within each 50 × 50 km region. (a) ERS-2. (b) Envisat. (c) GLAS Laser 2a. (d) ICESat/GLAS slope map. The GSFC V4 retracker was used for the radar results.

C. Comparison of Radar Data to the ICESat DEM

Comparing the full-rate (20 Hz) radar altimeter elevation measurements to an ICESat-derived DEM gives another measure of the accuracy of the radar-derived elevations. This has the advantage of using all the radar altimetry instead of only the data surrounding the crossovers, thus giving more information at regions away from the pole where the crossovers are sparser. The ICESat DEMs [22] used in this comparison are 1-km grids of Greenland and 500-m grids of Antarctica created using all the Laser 1 and Laser 2a ICESat data. Portions of these DEMs

were validated by comparing them to elevations retrieved from aircraft laser altimetry. For northwest Greenland, the differences were -41 ± 44 cm. For Marie Byrd Land in Antarctica, the differences were -8 ± 82 cm. An elevation residual is formed for each radar measurement by bilinearly interpolating the DEM to the geolocation of the radar measurement and then differencing that from the radar-derived elevation. Two sets of residuals are calculated: one using the Envisat elevations geolocated to the subsatellite point with no slope correction applied and one with the GSFC slope correction applied using (1). The sense of the residuals is always radar DEM elevation for direct comparison with the crossover results. The differences are then binned by slope. A 3σ iterative edit is performed for each slope bin, where σ is the standard deviation of the residual distribution within that slope bin, to remove bad data. Convergence is defined when σ changes by less than 2%.

IV. Results

A. Single Mission Results

Fig. 4 shows the precision of the four missions as a function of slope as measured by the standard deviations of the intramission crossover residuals for Greenland [Fig. 4(a)] and Antarctica [Fig. 4(b)]. For the ERS-2 and Envisat results, the GSFC range correction method was applied to correct for the slope-induced error. Laser 2a shows the highest precision of 14–15 cm up to 0.6° slopes for Antarctica and 16–20 cm over Greenland. The precision over Greenland for Laser 2a decreases to 50 cm at the highest slope bin and to 37 cm over Antarctica. Laser 1, in general, shows slightly degraded precision compared to Laser 2a with values varying from 20 to 52 cm. This is due to the less accurate pointing knowledge for Laser 1 as discussed in Section II-D. The degradation in laser precision at the higher slopes will decrease as better attitude solutions become available. The laser results also contain errors due to atmospheric forward scattering and saturation, which is highest over the flatter regions. Both of these alter the shape of the waveform. For saturated returns, ICESat's standard Gaussian fit processing is biased toward longer ranges, leading to low elevation estimates [20]. When forward scattering occurs, more signal occurs in the beginning of the return, leading to high elevation estimates. Therefore, the two effects can counteract each other. Laboratory-derived saturation corrections are now being calculated assuming no forward scattering. When this correction is applied to saturated data over the flat region of the Salar de Uyuni, it reduces the rms misfit between ICESat and the GPS-measured surface from 4.9 to 3.2 cm and the mean difference from -9.6 to -1.9 cm [21].

The radar results shown in Fig. 4 show a greater degradation with slope than the ICESat results. The precision of ERS-2 varies from 59 cm to 3.71 m. In contrast, the Envisat precision is better than ERS-2 varying from 27 cm to 2.06 m. The increase in precision for Envisat when compared with ERS-2 is due to the finer resolution of the Envisat fine-mode data compared to the ERS-2 ice-mode data. Each gate in the return waveform represents 46 cm in range for Envisat fine-mode data, whereas it represents 174 cm for the ERS-2 ice-mode data used in this paper.

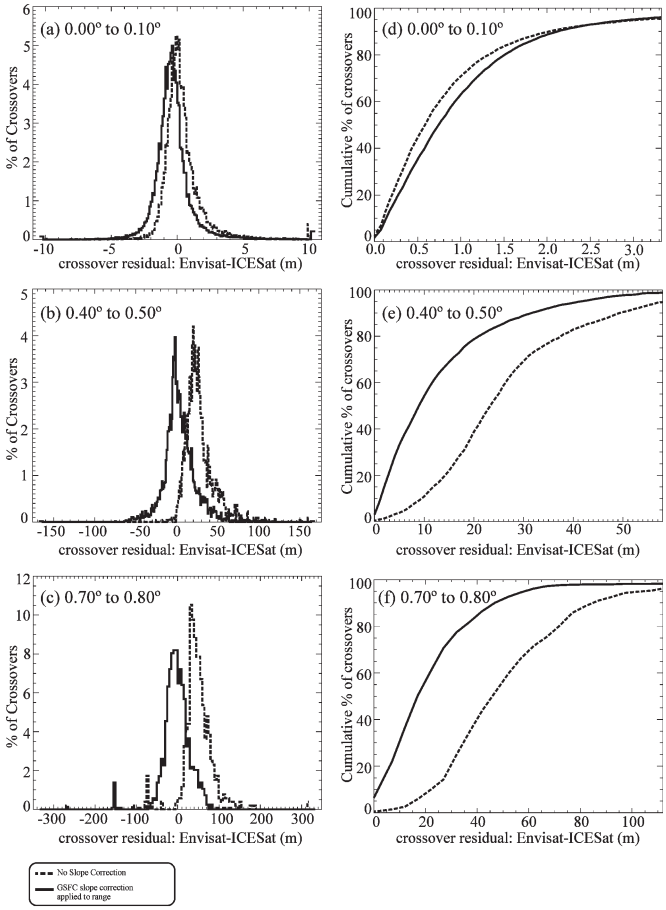

Fig. 6. Comparison of near-time-coincident Envisat/ICESat elevation retrievals showing the effect of slope on the Envisat retrievals and how the slope-induced error correction compensates for the error. (a)–(c) Histograms of the Envisat–GLAS elevation differences without any slope correction and with the GSFC range correction for different surface slopes. (d)–(f) Show the cumulative percent of crossovers for which the absolute value of the Envisat–GLAS residual is less than a given amount for the same surface slopes.

To show that the precision degradation with slope is not an artifact of the GSFC V4 retracker's fundamental function or the "tracker jitter" caused by switching from the single-ramp to double-ramp functions, we calculated the same statistics using both a 10% threshold retracker and only the data retracked with the single-ramp GSFC V4 retracker for ERS-2 over Greenland. These results are presented in Fig. 4(c), where the GSFC V4 results are repeated for direct comparison. The general trend is the same independent of which retracker is used. The threshold retracker results show the highest precision at the lower slopes, with the GSFC V4 single-ramp retrievals showing a higher precision than even the threshold retrievals at slopes higher than 1.0°. This is because the double ramp fits occur over the more irregular surfaces; thus, using only the single-ramp returns edits out the less precise data from the rougher surfaces. For the 10% threshold results and the "V4 all return" results, all returns that could be tracked with either a single or double ramp were used. We show ERS-2 data for this comparison because the GSFC V4 retracker chooses the single-ramp function for over 99% of the Envisat data. Therefore, "tracker jitter" is not a concern for Envisat results.

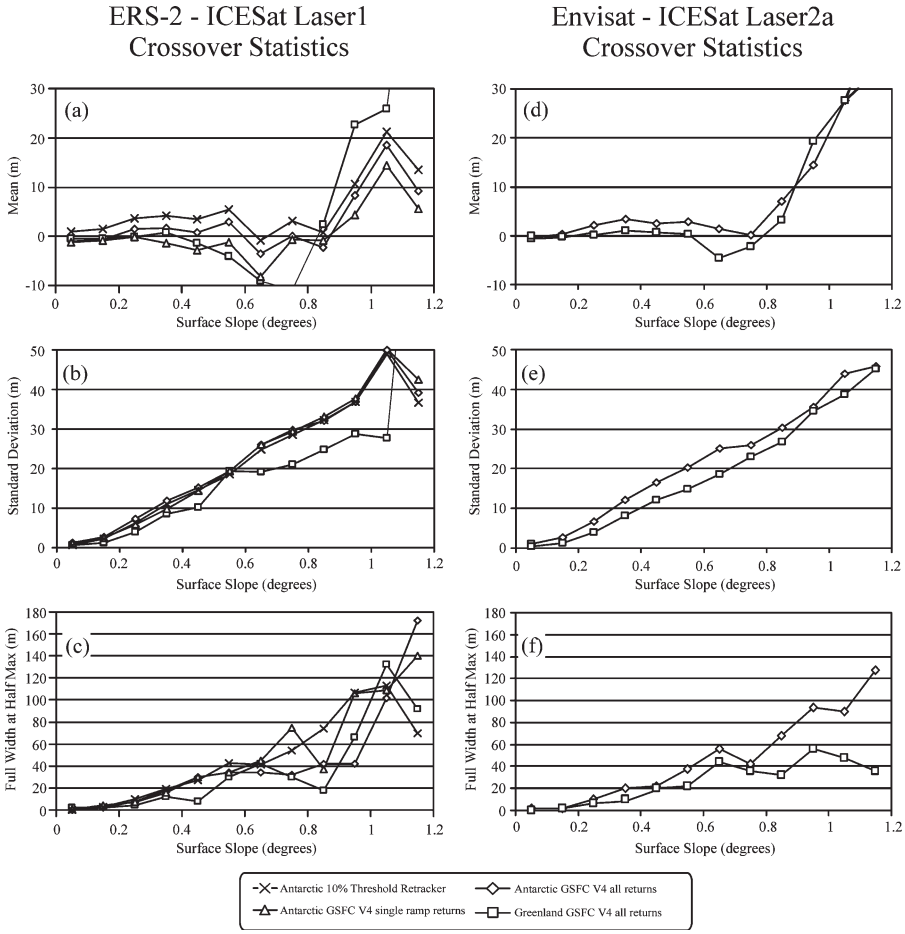

Fig. 7. Crossover residual statistics (radar–laser) between near-time-coincident passes as a function of surface slope. (a)–(c) ERS-2–Laser 1 statistics with the GSFC slope correction applied to ERS-2. Statistics for Antarctica are plotted for three different retracking scenarios, namely: 1) the GSFC V4 retracker with single-ramp returns only; 2) the 10% threshold retracker; and 3) the GSFC V4 retracker results using data from both single- and double-ramp returns. (d)–(f) Envisat–Laser 2a results with the GSFC V4 retracker and the GSFC slope correction applied to Envisat.

The geographic distribution of the altimeter-derived elevation precision over Antarctica is displayed in Fig. 5 for ERS-2, Envisat, and Laser 2a along with an Antarctic slope map derived from the ICESat DEM. The figure clearly shows the general correlation of precision with slope and the relative precision between the three altimeters. The improved precision of the ICESat-retrieved elevations over both ERS-2 and Envisat and the improvement in the Envisat results over those from ERS-2 by approximately a factor of 2 is clearly portrayed here. The lack of ICESat measurements over the ice shelves is due to our data selection criteria. Cloud cover attenuating the laser return causes the holes in the results over the coastal regions. The areas missing in the ERS-2 results are due to loss of data.

B. Radar–Laser Comparisons

A direct crossover comparison between the radar- and ICESat-retrieved elevations gives an estimate of the accuracy of the radar-derived elevations since the small laser footprint limits the amount of error in the laser-derived elevations even at the higher slopes. As discussed in Section II-C, the largest error in the radar altimetry elevations is due to the slope-induced error. Fig. 6 shows histograms of the Envisat–Laser 2a crossover residuals over three different surface slope intervals, namely: 1) 0.0° to 0.1°; 2) 0.4° to 0.5°; and 3) 0.7° to 0.8° for Antarctica. For each of these slope intervals, two different histograms are shown: one calculated without any correction for the radar slope-induced error and one applying the GSFC range correction.

The histograms without any slope correction show a one-sided non-Gaussian distribution with the peak location of the distribution increasing with slope. Since the radar always measures to the highest surface in the large beam-limited footprint (1.2–16 km), it returns elevations that are higher than the laser elevations retrieved from the small ∼70-m footprint. The slope correction causes the resultant crossover residual distributions to be centered closer to zero and to be double sided, having a more Gaussian shape. Fig. 6(d)–(f) shows the cumulative percent of Envisat data that agrees to within a given number of meters of ICESat elevations in an absolute sense. The abscissa is the absolute value of the difference between the Envisat- and ICESat-retrieved elevations. At any point on the abscissa if one draws a vertical line, the intersection of the vertical line with the curve shows what percent of the Envisat elevations agree to within the abscissa value to the ICESat elevations. Over flat regions, the slope correction causes an increase in the residual values probably due to inaccuracies in the DEMs used to calculate the slope correction. Over the 0.4° to 0.5° slopes,

TABLE II
NUMBER OF CROSSOVERS IN EACH BIN AND THE PERCENT USED WHEN ONLY USING CROSSOVERS RETRACKED WITH THE SINGLE-RAMP GSFC V4 RETRACKER FUNCTION

Surface Slope (deg)	Envisat - ERS-2 Antarctica Crossovers		ERS-2 - Laser 1 Antarctica Crossovers	
	total #	% single ramp V4	total #	% single ramp V4
0.0-0.1	37894	99.5	11795	99.8
0.1-0.2	44484	96.1	14403	95.9
0.2-0.3	16263	84.1	4895	85.6
0.3-0.4	7652	74.2	2250	79.3
0.4-0.5	4235	74.0	1316	68.8
0.5-0.6	2475	70.8	939	60.9
0.6-0.7	1621	70.7	444	61.9
0.7-0.8	1254	67.7	325	64.6
0.8-0.9	764	63.2	267	74.9
0.9-1.0	408	55.9	139	51.1
1.0-1.1	231	60.6	81	60.5
1.1-1.2	150	50.0	32	70.0

only 10% of the crossover residuals agree to within 10 m of ICESat results when no correction is applied in contrast to 60% when the NASA range correction is applied. At 0.7° to 0.8° slope, the contrast is even larger, with 5% of the data agreeing to within 20 m of ICESat results when no correction is applied and 60% when the NASA range correction is applied.

Fig. 7 summarizes the crossover residual distributions for radar–laser comparisons, showing the mean, standard deviation, and full-width at half-maximum (FWHM) amplitude for ERS-2–Laser 1 and Envisat–Laser 2a crossover distributions as a function of surface slope.

For ERS-2–Laser 1 Antarctica crossovers [Fig. 7(a)–(c)], three different cases are shown, all using the GSFC range correction method to correct for the slope-induced error, but different retracking: 1) the GSFC V4 algorithm that allows switching between single- and double-ramp fits; 2) the GSFC V4 algorithm using only returns that fit a single ramp; and 3) a 10% threshold retracker. The mean value of the distribution is lowest in magnitude, indicating closer agreement with ICESat, when the full NASA V4 retracker is used up to 0.9° surface slope over Antarctica. The spread of the distributions over Antarctica, as measured by the standard deviations, follow the same trend for all three retrackers varying from 60 cm to 50 m with surface slope. The single-ramp GSFC V4 retracker shows the narrowest distribution, followed by the threshold retracker and the full GSFC V4 retracker through slopes of 0.5°.

For Greenland, we show only the NASA V4 retracker. The standard deviation increases with slope up to 40 m at 1° but is consistently lower for Greenland than for Antarctica. The FWHM results are similar in trend to those of the standard deviation until 0.6° slope, where they increase significantly and diverge from each other. A 3σ convergent edit was performed in calculating the mean and the standard deviation, where σ was the standard deviation of the crossovers in the associated slope bin. From 2% to 5% of the data were edited out. No edits were performed on the data before the calculation of the FWHM. Table II shows the number of data points used in each slope bin in the ERS-2–Laser 1 distribution, and the percentage of the data points kept when only the single-ramp functional fit data were used. As expected, the double-ramp returns are mostly in the rougher sloping regions.

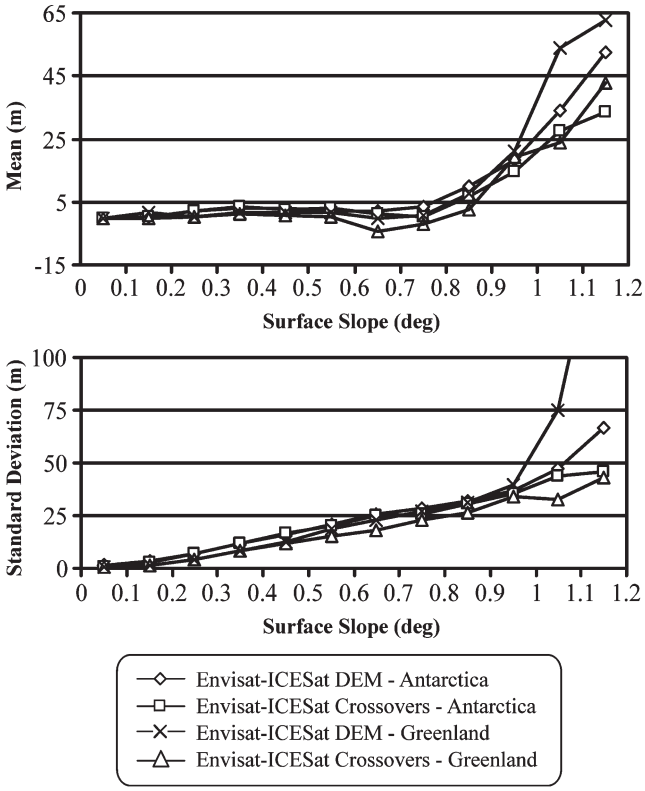

Fig. 8. Comparison of Envisat-derived elevations to the ICESat/GLAS DEMs for Antarctica and Greenland. The GSFC V4 retracker and slope correction were applied to the Envisat data. The Envisat–Laser 2a crossover statistics are replotted here for comparison.

In summary, the slope correction decreases the mean of the radar–laser residuals, but the standard deviation is not markedly affected. The increase in standard deviation with slope is not surprising since at 0.6°, the antenna has reached the 3-dB attenuation point and decreases exponentially from there, causing significant power attenuation beyond a 0.6° surface slope. This makes it more difficult to decipher the mean surface location on the return waveform, causing the elevation retrievals to exhibit more noise.

For the Envisat–Laser 2a comparison [Fig. 7(d)–(f)], the complete GSFC V4 retracker is used in all cases. The mean difference between Envisat–Laser 2a over Greenland varies from -9 ± 52 cm for slopes less than 0.1° to 2.7 ± 26 m at slopes up to 0.9°. Comparable statistics over Antarctica show the trends are the same, but the actual numbers are higher, ranging from -40 ± 98 cm for slopes less than 0.1° to 6 ± 30 m at slopes up to 0.9°. Above 0.9° slope, the agreement becomes considerably worse. This is probably due to errors in the DEM used to calculate the slope correction.

The comparison of the Envisat radar results to the ICESat DEM is presented in Fig. 8 along with the crossover results from Fig. 7 for comparison. The GSFC V4 retracker and slope-induced range correction were applied for the Envisat retrievals. Both the mean difference and standard deviation for comparisons with the DEM are similar to the crossover results until 0.9° slopes. This infers that the DEM in the higher sloping regions does not represent the actual data as well as over the

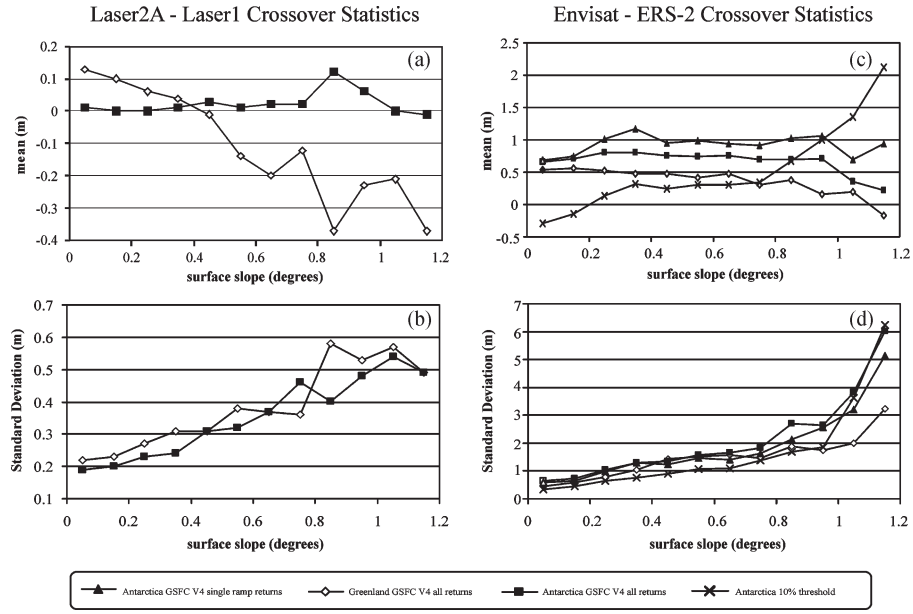

Fig. 9. Ice sheet crossover residual statistics. (a) and (b) Laser 2a–Laser 1. (c) and (d) Envisat–ERS-2. For Envisat-ERS-2 over Antarctica, results are shown using three different retracking scenarios, namely: 1) the GSFC V4 retracker with single-ramp returns only; 2) the 10% threshold retracker; and 3) the GSFC V4 retracker results using data from both single- and double-ramp returns.

lower slopes. The DEM is calculated by fitting a biquadratic surface to all data within a given region around the grid node. These results infer that at the larger slopes, the actual surface does not fit as well to a biquadratic function, causing smoothing in the DEM.

These radar–laser comparisons show that the radar measurements differ significantly from the near-time-coincident laser measurements mostly due to our inability to model the slope-induced error correctly, signifying that we cannot define accurately enough where the radar is measuring to within the large beam-limited footprint.

C. Envisat–ERS-2 and Laser 2a–Laser 1 Comparisons

The two time periods used in this paper are approximately six months apart. In Fig. 9, we show the differences between Laser 2a and Laser 1 [Fig. 9(a) and (b)] and between Envisat and ERS-2 [Fig. 9(c) and (d)] as exemplified by the mean and standard deviation of the crossover distributions. The GSFC slope-induced range correction was applied to the Envisat and ERS-2 retrievals. The Laser 2a–Laser 1 crossover distributions over Antarctica have a mean of 0–3 cm except between 0.8° and 0.9° slope where it increases to 10 cm. The crossover distribution mean over Greenland shows a general downward trend starting at +13 cm and decreasing to −38 cm at the higher slopes, which may be indicative of elevation changes in the higher sloping regions over the six months. The standard deviation generally increases in slope from 20 to 60 cm over both continents. The mean values of the Envisat–ERS-2 crossover distributions using the GSFC V4 retracker show a downward trend over both continents with slope varying from 66 to 22 cm over Antarctica and a slightly larger variation going from 55 to −17 cm over Greenland. The standard deviations vary with slope from 65 cm to 6 m for Antarctica and from 44 cm to 3 m over Greenland. To determine the dependence of the Envisat–ERS-2 comparison on retracker type, the results from both the 10% threshold retracker and using only the single-ramp returns from the GSFC V4 retracker are also shown in Fig. 9(c) and (d) for Antarctica. The mean results using the threshold retracker do not follow the same trend and show a smaller value than the other retrackers up to 0.7°, where it increases with slope reaching a mean difference of 2.1 m at 1.1° to 1.2°. The standard deviations for the threshold retracker distribution are lower than the other retracker results until 0.9° slope, where the tightest distribution is shown by the GSFC V4 retracker results. This shows that the results are definitely retracker dependent but does not definitively show which retracker produces more precise results.

V. Summary

ICESat-derived elevations are significantly more accurate and of higher precision than those derived from the radar altimeters. Therefore, ICESat can be used to determine the general magnitude of the residual error in the ERS-2- and Envisat-derived elevations. The ICESat data used for this paper were of a preliminary nature and still include errors due to imprecise pointing knowledge, saturation, and atmospheric forward scattering. Corrections for saturation and atmospheric forward scattering are being worked on by the ICESat science team, as is improvement in the pointing knowledge. This paper shows the precision of ICESat-retrieved elevations over the ice sheets to vary from 14 to 50 cm as a function of surface slope.

The radar altimeter-derived elevation accuracy is driven by the slope-induced error. The results show that Envisat data have improved precision and accuracy over ERS-2 data as expected by the finer resolution range bins used. In regions of very low slope, the Envisat data agree to within 9 cm ± 0.5 m with the ICESat results over Greenland. The GSFC range correction for the slope-induced error corrects for a good portion of the error at slopes less than 0.9°. However, the correction is not accurate enough to combine the laser and radar measurements

in elevation change studies. The laser–radar results show, as expected, that the threshold retracker gives less accurate absolute elevations than the GSFC V4 retracker but has better internal consistency as evidenced by the lower noise levels.

ACKNOWLEDGMENT

The authors would like to thank M. Beckley for his help in preparing the graphics.

REFERENCES

[1] H. J. Zwally, A. C. Brenner, J. A. Major, R. A. Bindschadler, and J. G. Marsh, "Growth of Greenland ice sheet: Measurement," *Science*, vol. 246, no. 4937, pp. 1587–1589, Dec. 1989.

[2] D. J. Wingham, A. J. Ridout, R. Scharroo, R. J. Arthern, and C. K. Shum, "Antarctic elevation change from 1992 to 1996," *Science*, vol. 282, no. 5388, pp. 456–458, Oct. 1998.

[3] C. H. Davis, "Elevation change of the Antarctic ice sheet, 1995–2000, from ERS-2 satellite radar altimetry," *IEEE Trans. Geosci. Remote Sens.*, vol. 42, no. 11, pp. 2437–2445, Nov. 2004.

[4] H. J. Zwally *et al.*, "ICESat's laser measurements of polar ice, atmosphere, ocean and land," *J. Geodyn.*, vol. 34, no. 3/4, pp. 405–445, 2002.

[5] J. L. Bamber, S. Ekholm, and W. B. Krabill, "The accuracy of satellite radar altimeter data over the Greenland ice sheet determined from airborne laser data," *Geophys. Res. Lett.*, vol. 25, no. 16, pp. 3177–3180, 1998.

[6] J. L. Bamber and J. L. Gomez-Dans, "The accuracy of digital elevation models of the Antarctic continent," *Earth Planet. Sci. Lett.*, vol. 237, no. 3/4, pp. 516–523, Sep. 2005.

[7] K. J. Quinn and T. A. Herring, "Atmospheric delay correction to GLAS laser altimeter ranges," *GLAS Algorithm Theoretical Basis Document*, 2000. [Online]. Available: http://www.csr.utexas.edu/glas/atbd.html

[8] H. A. Phillips, J. Ridgway, and B. Minster, *Tidal Corrections, Geoscience Laser Altimeter System (GLAS) Algorithm Theoretical Basis Document*, 1999. Version 2.0, unpublished. [Online]. Available: http://www.csr.utexas.edu/glas/atbd.html

[9] H. J. Zwally and A. C. Brenner, "Ice sheet dynamics and mass balance," in *Satellite Altimetry and Earth Sciences*, L. L. Fu and A. Cazenave, Eds. New York: Academic, 2001, pp. 351–369.

[10] J. K. Ridley and K. C. Partington, "A model of satellite radar altimeter returns from ice sheets," *Int. J. Remote Sens.*, vol. 9, no. 4, pp. 601–624, 1988.

[11] C. H. Davis and V. I. Poznyak, "The depth of penetration in Antarctic firn at 10 GHz," *IEEE Trans. Geosci. Remote Sens.*, vol. 31, no. 5, pp. 1107–1111, Sep. 1993.

[12] J. L. Bamber, "Ice sheet altimeter processing scheme," *Int. J. Remote Sens.*, vol. 15, no. 4, pp. 925–938, 1994.

[13] C. H. Davis, "A robust threshold retracking algorithm for measuring ice-sheet surface elevation change from satellite radar altimeters," *IEEE Trans. Geosci. Remote Sens.*, vol. 35, no. 4, pp. 974–979, Jul. 1997.

[14] ——, "A surface and volume scattering retracking algorithm for ice sheet satellite altimetry," *IEEE Trans. Geosci. Remote Sens.*, vol. 31, no. 4, pp. 811–818, Jul. 1993.

[15] R. J. Arthern, D. J. Wingham, and A. L. Ridout, "Controls on ERS altimeter measurements over ice sheets: Footprint-scale topography, backscatter fluctuations, and the dependence of microwave penetration depth upon satellite orientation," *J. Geophys. Res.*, vol. 106, no. D24, pp. 33 471–33 484, Dec. 2001.

[16] D. C. Bilitza, C. Koblinsky, B. Beckley, S. Zia, and R. Williamson, "Using IRI for the computation of ionospheric corrections for altimeter data analysis," *Adv. Space Res.*, vol. 15, no. 2, pp. 113–119, 1995.

[17] A. C. Brenner, R. A. Bindschadler, R. H. Thomas, and H. J. Zwally, "Slope-induced errors in radar altimetry over continental ice sheets," *J. Geophys. Res.*, vol. 88, no. 3, pp. 1617–1623, 1983.

[18] S. D. Luthcke, D. Rowlands, T. Williams, and M. Sirota, "Reduction of ICESat systematic geolocation errors and the impact on ice sheet elevation change detection," *Geophys. Res. Lett.*, vol. 32, no. 21, L21S05, Nov. 2005.

[19] A. C. Brenner *et al.*, *Derivation of Range and Range Distributions From Laser Pulse Waveform Analysis for Surface Elevations, Roughness, Slope, and Vegetation Heights, Geoscience Laser Altimeter System (GLAS) Algorithm Theoretical Basis Document*, 2004. Version 4.1, unpublished. [Online]. Available: http://www.csr.utexas.edu/glas/atbd.html

[20] J. Abshire *et al.*, "Geoscience Laser Altimeter System (GLAS) on the ICESat mission: On-orbit measurement performance," *Geophys. Res. Lett.*, vol. 32, no. 21, L21S02, Nov. 2005.

[21] H. A. Fricker *et al.*, "Assessment of ICESat performance at the Salar de Uyuni, Bolivia," *Geophys. Res. Lett.*, vol. 32, no. 21, L21S06, Nov. 2005.

[22] J. P. DiMarzio *et al.*, *Digital Elevation Models of the Antarctic and Greenland Ice Sheets From ICESat*, Dec. 2005. EOS C51B-0276.

Anita C. Brenner received the B.S. degree in aerospace engineering from the University of Cincinnati, Cincinnati, OH, in 1970 and the M.S. degree in electrical engineering with a major in biomedical engineering and a minor in guidance and control from the University of Maryland, College Park, in 1975.

She has been involved in satellite altimetry since 1976, developing algorithms to map the oceans, land, ice sheets, and river changes using radar and laser altimetry. She is currently a Program Manager with Science Systems and Applications, Inc., Lanham, MD, managing programs at the National Aeronautics and Space Administration (NASA)/Goddard Space Flight Center in support of Earth science. She has been supporting the use of radar and laser altimetry for polar ice analysis since 1979 and has more than 20 referred publications using altimetry for studying the ice sheets, oceans, and lakes. She has been a member of the algorithm development teams and calibration and validation teams for NASA and European Space Agency laser and radar altimeters, most recently playing a major role in developing the ice sheet elevation retrieval algorithms for the Geoscience Laser Altimeter System.

Ms. Brenner is a member of Tau Beta Pi, the International Glaciological Society, and the American Geophysical Union. She has received NASA Group Achievement Awards for supporting the TOPEX, Geosat, and ICESat missions.

John P. DiMarzio received the B.S. degree in physics from the University of Maryland, College Park, in 1990.

He has been extensively involved in satellite radar and laser altimetry since 1989 and is currently a Chief Systems Engineer for Stinger Ghaffarian Technologies, Inc., Greenbelt, MD, on a National Aeronautics and Space Administration (NASA)/Goddard Space Flight Center contract supporting the ICESat mission and satellite radar altimetry studies. He has six referred publications using altimetry for studying the ice sheets.

Mr. DiMarzio is a member of the American Geophysical Union. He has received NASA Group Achievement Awards for supporting the ICESat mission.

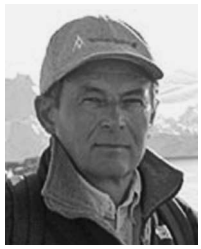

H. Jay Zwally received the B.S. degree in mechanical/aeronautical engineering from Drexel University, Philadelphia, PA, in 1961 and the Ph.D. degree in physics with a minor in mathematics from the University of Maryland, College Park, in 1969.

He has been extensively involved in glaciology and polar research since 1971. He pioneered the use of ocean radar altimeters for mapping ice sheet topography and studies of mass balance. Since 1979, he has been a leading scientist with the National Aeronautics and Space Administration (NASA)/Goddard Space Flight Center, Greenbelt, MD, promoting satellite laser altimetry for ice sheet mass balance studies, leading to the launch of the Ice Cloud and Land Elevation Satellite (ICESat) in 2003. Currently, he is the ICESat Project Scientist and a Member of the science teams for the Geoscience Laser Altimeter System, the Mars Orbiting Laser Altimeter, and ENVISAT and CRYOSAT Calibration/Validation. He has had more than 100 referred publications in glaciology, polar research, climate science, and physics. His recent research includes leading a comprehensive analysis of the mass balance of the Greenland and Antarctic ice sheets and ice shelves, the discovery of the melt-acceleration effect on the flow of the Greenland ice sheet, and the first comprehensive mapping of sea ice freeboard and thickness distributions.

Dr. Zwally is a member of the International Glaciological Society and the American Geophysical Union. He was the recipient of NASA's Goddard Award of Merit for Outstanding Contributions and Scientific Leadership (2005), the Outstanding Scientific Achievement Award (1996), and the Goddard's Exceptional Performance Award for leadership in establishing a cryospheric research program (1978).